

1000 JF

(12)

AFRPL-TR-80-66

FEBRUARY 1981

**AIR FORCE ROCKET PROPULSION LABORATORY**

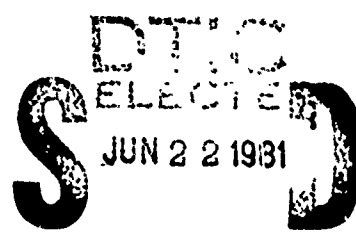
Director of Laboratories  
Air Force Systems Command  
Moffett AFB, Ca 93523

AD A100517

**SPECIAL REPORT**

**A SURFACE DAMAGE INVESTIGATION  
ON UNIAXIAL TENSILE TEST SPECIMENS  
PREPARED BY  
COMMON CUTTING METHODS**

THOMAS J. C. CHEW  
DALE A. WELLS



A

DTIC FILE COPY

**APPROVED FOR PUBLIC RELEASE • DISTRIBUTION UNLIMITED**

## NOTICES

When U.S. Government drawings, specifications, or other data are used for any purpose other than a definitely related Government procurement operation, the Government thereby incurs no responsibility nor any obligation whatsoever, and the fact that the Government may have formulated, furnished or in any way supplied the said drawings, specifications, or other data is not to be regarded by implication or otherwise, or in any manner licensing the holder or any other person or corporation or conveying any rights for permission to manufacture, use or sell any patented invention that may in any way be related thereto.

## FOREWORD

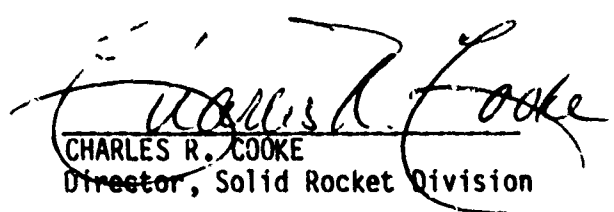
This report describes the work conducted by the Mechanical Behavior and Aging Section (MKB) of the Air Force Rocket Propulsion Laboratory, Edwards AFB, California 93523 under Job Order No. 573013NE.

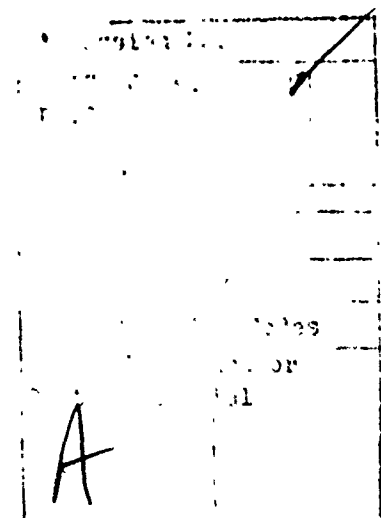
This technical report is approved for release and distribution in accordance with the distribution statement on the cover and on the DD Form 1473.

  
THOMAS J.C. CHEW  
Project Manager

  
ROBERT L. GEISLER  
Chief, Propellant Development Branch

FOR THE COMMANDER

  
CHARLES R. COOKE  
Director, Solid Rocket Division



## UNCLASSIFIED

SECURITY CLASSIFICATION OF THIS PAGE (When Data Entered)

REPORT DOCUMENTATION PAGE		READ INSTRUCTIONS BEFORE COMPLETING FORM
1. REPORT NUMBER AFRPL-TR-80-66	2. GOVT ACCESSION NO. AD-A100517	3. RECIPIENT'S CATALOG NUMBER
4. TITLE (and Subtitle) A Surface Damage Investigation on Uniaxial Tensile Test Specimens Prepared by Common Cutting Methods		5. TYPE OF REPORT & PERIOD COVERED Special Report 6. PERFORMING ORG. REPORT NUMBER 15 Jan 79 - 15 Jul 84
7. AUTHOR(s) Thomas J.C. Chew Dale A. Wells	7. CONTRACTOR REPORT NUMBER(s)	
8. PERFORMING ORGANIZATION NAME AND ADDRESS Air Force Rocket Propulsion Laboratory/MKPB Edwards AFB, CA 93523	10. PROGRAM ELEMENT PROJECT, TASK AREA & WORK UNIT NUMBERS Program Element 62302F Project 5730 Task 13 JON: 573013NE	
11. CONTROLLING OFFICE NAME AND ADDRESS 1615730 11 11	12. REPORT DATE February 1981	
14. MONITORING AGENCY NAME & ADDRESS (if different from Controlling Office)	13. NUMBER OF PAGES 141	
15. SECURITY CLASS. (or milia report) Unclassified	15a. DECLASSIFICATION/DOWNGRADING SCHEDULE NA	
16. DISTRIBUTION STATEMENT (of this Report) Approved for public release; distribution unlimited		
17. DISTRIBUTION STATEMENT (of the abstract entered in Block 20, if different from Report)		
18. SUPPLEMENTARY NOTES		
19. KEY WORDS (Continue on reverse side if necessary and identify by block number) Propellant Cutting Propellant Surface Damage Propellant Cutting Techniques Propellant Test Specimen Preparation      Test Specimen Preparation Damage		
20. ABSTRACT (Continue on reverse side if necessary and identify by block number) An experimental investigation was conducted to evaluate propellant test specimen surface damage caused by three common cutting methods, each operated at three different speeds. The three methods were guillotine cutting, sawing and milling. For each set of cutting conditions (method and speed), six specimens were obtained. Three of these specimens were subjected to surface damage evaluation using a scanning electron microscope. The remaining three specimens were (over)		

~~UNCLASSIFIED~~

SECURITY CLASSIFICATION OF THIS PAGE(When Data Entered)

subjected to uniaxial tensile testing. The effects of each set of cutting conditions on specimen surface damage and the resulting mechanical property change were analyzed. It was found that saw-cut and mill-cut propellant surfaces were similar in appearance and relatively smooth, whereas guillotine-cut surfaces were more rugged and had sustained more damage as manifested in extracted, dislocated and fractured particles. However, no significant difference in uniaxial tensile properties was found between the three cutting methods or between the three cutting speeds in each cutting method. It is believed that the absence of bonding agent in the test propellant (TP-H1011) is a significant factor in the insensitivity of test specimens mechanical properties to their surface damage condition.

~~UNCLASSIFIED~~

SECURITY CLASSIFICATION OF THIS PAGE(When Data Entered)

REPORT DOCUMENTATION PAGE		READ INSTRUCTIONS BEFORE COMPLETING FORM
1. REPORT NUMBER	2. GOVT ACCESSION NO.	3. RECIPIENT'S CATALOG NUMBER
4. TITLE (and Subtitle)		5. TYPE OF REPORT & PERIOD COVERED
		6. PERFORMING ORG. REPORT NUMBER
7. AUTHOR(s)		8. CONTRACT OR GRANT NUMBER(s)
9. PERFORMING ORGANIZATION NAME AND ADDRESS		10. PROGRAM ELEMENT, PROJECT, TASK AREA & WORK UNIT NUMBERS
11. CONTROLLING OFFICE NAME AND ADDRESS		12. REPORT DATE
		13. NUMBER OF PAGES
14. MONITORING AGENCY NAME & ADDRESS (if different from Controlling Office)		15. SECURITY CLASS. (of this report)
		15a. DECLASSIFICATION/DOWNGRADING SCHEDULE
16. DISTRIBUTION STATEMENT (of this Report)		
17. DISTRIBUTION STATEMENT (of the abstract entered in Block 20, if different from Report)		
18. SUPPLEMENTARY NOTES		
19. KEY WORDS (Continue on reverse side if necessary and identify by block number)		
20. ABSTRACT (Continue on reverse side if necessary and identify by block number)		

## PREFACE

This technical report summarizes the work performed on the Specimen Surface Damage Investigation Task under the in-house Solid Propellant Mechanical Behavior Programs at the AFRPL between 15 January 1979 and 15 June 1980. No previous technical reports have been published on this work.

The authors wish to acknowledge those people who proved invaluable to the completion of this effort at the AFRPL. Lt. Terry Kling, as the Development Engineer, was responsible for fulfilling the overall test plan. Mr. Thomas Owens skillfully took all electron microscope photographs of cut specimen surfaces used in this investigation. MSgt Rex Thompson, Mr. Kelly Palmer and Mr. Larry Wilburn patiently prepared all test specimens. The mechanical property tests were faithfully performed by the collective effort of Mr. Harold Anderson, Mr. Paul J. Markle and Mr. Aaron Perea. Finally, special thanks to Ms. Shelley Herman for typing the drafts of this report.

## TABLE OF CONTENTS

	<u>PAGE</u>
1. INTRODUCTION	7
1.1 Background and Task Objective	7
1.2 Scope of Work	8
1.2.1 Test Specimens Preparation	8
1.2.2 Unaxial Tensile Properties Evaluation	8
1.2.3 Electron Microscope Surface Examination	9
1.2.4 Block-to-block Tensile Properties Variation Evaluation	9
2. EXPERIMENTAL PROCEDURES	10
2.1 Propellant Specimen Cutting Techniques	10
2.1.1 Cutting by Guillotine	10
2.1.2 Cutting by Circular Saw	10
2.1.3 Cutting by Milling Machine	11
2.1.4 Cutting by Die Cutter	11
2.2 Uniaxial Tensile Test	12
2.3 Electron Microscope Surface Examination	13
3. DATA REDUCTION AND ANALYSIS PROCEDURES	13
3.1 Reduction of Uniaxial Tensile Test Data	13
3.2 Analysis of Uniaxial Tensile Test Data	17
3.3 Analysis of Propellant Surface Photographs	19
4. EXPERIMENTAL RESULTS AND DISCUSSION	19
4.1 Uniaxial Tensile Tests	19
4.2 Electron Microscope Surface Examination	30
4.3 Interpretation of Test Results	36
5. CONCLUSIONS AND RECOMMENDATIONS	36
6. REFERENCES	37

LIST OF FIGURES

<u>FIGURE</u>		<u>PAGE</u>
1.	Control Room for Remote Cutting of Propellant	38
2.	Guillotine Cutter, Front View	39
3.	Guillotine Cutter, Rear View	40
4.	Circular Saw for Propellant Cutting	41
5.	Propellant Milling Machine	42
6.	Press and Die Cutter for JANNAF Uniaxial Tensile Test Specimen	43
7.	Typical Load Displacement Curve with Data Reduction Illustration	14
8.	Typical Stress vs. Strain Representation of Test Data	16
9.	Typical Stress vs. Strain Curve with Data Reduction Illustration	16
10.	Comparison of Stress Capability Between Cutting Methods and Between Cutting Speeds	25
11.	Comparison of Strain Capability Between Cutting Methods and Between Cutting Speeds	26
12.	Block-to-Block Variation in Stress Capability	28
13.	Block-to-Block Variation in Strain Capability	29
14.	SEM Photographs of Mill-Cut Surfaces at $.741 \times 10^{-3}$ m/s (1.75 in/min) Feed Rate	44/45
15.	SEM Photographs of Mill-Cut Surfaces at $2.01 \times 10^{-3}$ m/s (4.75 in/min) Feed Rate	46/47
16.	SEM Photographs of Mill-Cut Surfaces at $3.07 \times 10^{-3}$ m/s (7.25 in/min) Feed Rate	48/49
17.	SEM Photographs of Guillotine-Cut Surfaces at 0.414 MPa (60 psi) Operating Pressure	50/51
18.	SEM Photographs of Guillotine-Cut Surfaces at 0.621 MPa (90 psi) Operating Pressure	52/53
19.	SEM Photographs of Guillotine-Cut Surfaces at 0.827 MPa (120 psi) Operating Pressure	54/55

LIST OF FIGURES (CONT)

<u>FIGURE</u>		<u>PAGE</u>
20.	SEM Photographs of Saw-Cut Surfaces at $1.06 \times 10^{-3}$ m/s (2.5 in/min) Feed Rate	56/57
21.	SEM Photographs of Saw-Cut Surfaces at $2.54 \times 10^{-3}$ m/s (6 in/min) Feed Rate	58/59
22.	SEM Photographs of Saw-Cut Surfaces at $4.23 \times 10^{-3}$ m/s (10 in/min) Feed Rate	60/61

## LIST OF TABLES

TABLE	PAGE
1. Test Specimen Preparation Summary	9
2. Uncorrected Uniaxial Tensile Test Results	20/21
3. Corrected Uniaxial Tensile Test Results	22/23
4. Block-to-Block Variation of Uniaxial Tensile Properties (Milling at 1000 rpm)	27
5. SEM Results - Mill-Cut Surfaces	31
6. SEM Results - Guillotine-Cut Surfaces	32
7. SEM Results - Saw-Cut Surfaces	33
8. SEM Results - Comparison Between Cutting Methods	35

## 1. INTRODUCTION

### 1.1 Background and Task Objective

In recent years, several researchers working on solid propellant mechanical behavior have reported significant strain dependency of the relaxation modulus (References 1, 2 and 3). Usually the larger the strain imposed on the propellant test specimen, the lower the relaxation modulus obtained. This strain dependency is believed to be the result of "strain damage" incurred in the test specimen. It is easy to see that cutting and handling will distort (or strain) the propellant, especially when the specimen is thin. When the specimen is subjected to a tensile load during testing, it is strained further causing further "strain damage". At low strain level, the predominant mode of damage is believed to be micro-fissuring of the polymer, especially in regions adjacent to the filler particles. As strain level increases, dewetting of filler particles would become more prevalent.

"Strain damage" incurred in the test specimen as it is being strained during testing is unavoidable and does reflect a realistic propellant phenomenon in solid propellant motors. "Strain damage" due to specimen preparation and handling, however, is an artifact which can be and should be minimized. Francis et. al. at Chemical Systems Division (Reference 2) conducted tests with large cast propellant specimens that required neither cutting nor machining. They found that modulus values at 0.5-percent strain are nearly three times greater than those at 5-percent strain--a dramatic demonstration of the effect of "strain damage" due to specimen preparation and handling. Anderson et. al. at the Thiokol/Wasatch Division (Reference 3) had evaluated an improved method for test specimen preparation. They used the combination of a specially designed "miter box" and a jeweler's saw having a 0.397-mm (1/64-in.) thick blade. Their test results showed that, at 2 percent

strain, significantly higher (approximately 25 percent) relaxation modulus values were obtained with specimens prepared by the improved method as compared to those prepared using a guillotine.

Since test specimen preparation technique has a significant effect on the experimentally determined relaxation modulus, it is natural to ask whether the same is true for mechanical property values obtained from uniaxial tensile constant strain rate test. This test is widely used by the solid propellant contractors in their propellant development efforts, and test specimen preparation technique used is also widely varied among these contractors. Uniaxial tensile test data are invariably found in contractor proposals on propellant development programs. In order to compare data from different bidders intelligently, one must know and take into account the effect of specimen preparation technique on test results. It is to this end that the work described in this report was dedicated.

## 1.2 Scope of Work

1.2.1 Test Specimens Preparation - A total of 27 JANNAF Class C uniaxial tensile test specimens was prepared using three common propellant cutting methods. Three 1-gallon blocks of TP-H1011 propellant were used for this effort. Each block was reserved for one method only. The three cutting methods were (1) a guillotine operated at three slicing cylinder set pressures, (2) a circular saw ran at 350 revolutions per minute in conjunction with three propellant feed rates, and (3) a milling head ran at 1,000 revolutions per minute also with three different propellant feed rates. The scope of the test specimen preparation effort is summarized in Table 1.

1.2.2 Uniaxial Tensile Properties Evaluation - Twenty-seven uniaxial tensile tests were conducted with the test specimens described in Paragraph 1.2.1 above. All tests were conducted at 25°C (77°F) test

TABLE 1. TEST SPECIMEN PREPARATION SUMMARY

Cutting Method	Cutter Speed, rpm	Feed Rate m/s x10 <sup>-3</sup> (in/min)	Set Pressure, MPa (psi)	Number of Specimens
Guillotine	N/A	N/A	0.414 (60)	3
Guillotine	N/A	N/A	0.621 (90)	3
Guillotine	N/A	N/A	0.827 (120)	3
Circular Saw	350	1.06 (2.5)	N/A	3
Circular Saw	350	2.54 (6)	N/A	3
Circular Saw	350	4.23 (10)	N/A	3
Milling	1000	0.74 (1.75)	N/A	3
Milling	1000	2.01 (4.75)	N/A	3
Milling	1000	3.07 (7.25)	N/A	3

temperature and  $0.847 \times 10^{-3}$  m/s (2.0 in/min) crosshead speed. Test data were reduced to yield the initial modulus and the stress and strain values at the maximum force point, the maximum stress point and the rupture point.

1.2.3 Electron Microscope Surface Examination - Propellant cut surfaces resulted from using each of the nine cutting method/cutting speed combinations were photographed using a scanning electron microscope (SEM) at three different magnifications, namely 30X, 150X and 300X. This was done to detect visual differences in surface condition resulting from using different cutting techniques. A profile picture of each cut surface was also photographed at 150X magnification. In addition, some mapping with the SEM at 150X magnification was done to aid identification of filler particles on the propellant surface.

1.2.4 Block-to-Block Tensile Properties Variation Evaluation - To access the extent of inherent tensile property variation between the three

blocks of propellant used in this study, four uniaxial tensile test specimens were obtained from a single slab of each propellant block. The propellant slabs were all prepared the same way by milling at 1000 rpm milling head speed and  $2.01 \times 10^{-3}$  m/s (4.75 in/min) feed rate. A total of 12 tests were conducted with these specimens at a constant 25°C (77°F) test temperature and  $0.847 \times 10^{-3}$  m/s (2 in/min) crosshead rate.

## 2. EXPERIMENTAL PROCEDURES

### 2.1 Propellant Cutting Methods

JANNAF uniaxial tensile Class C propellant test specimens used in this program were prepared as described in the following subsections. All propellant cutting operations were remotely controlled, and were monitored with a closed circuit television system as shown in Figure 1.

2.1.1 Cutting by Guillotine - These test specimens were prepared by slicing off 1/2-inch thick slabs from a 1-gallon block of propellant using an in-house manufactured guillotine cutter shown in Figures 2 and 3. This guillotine was equipped with a Parker-Hannif hydraulically operated main slicing cylinder, which has an adjustable operating pressure range. The guillotine blade measured 203 mm (8 in.) wide and 9.53 mm (3/8 in.) thick, and had a cutting edge tapered (14°) on the near side. Guillotine operating pressures of 0.414 MPa (60 psi), 0.621 MPa (90 psi) and 0.827 MPa (120 psi) were used for propellant slicing. Care was taken to insure that the two sides of each slab were cut at the same pressure.

2.1.2 Cutting by Circular Saw - These specimens were prepared by sawing off 1/2-inch thick slabs from a 1-gallon block of propellant, using a circular saw operating at 350 rpm. As shown in Figure 4, a Blue Chip Manufacturing Company saw Model 3505L was used in conjunction with a 508 mm (20 in.) diameter, 1.58 mm (1/16 in.) thick Simonds Style CT-3 saw blade. The

teeth of this blade were each carbide tipped, approximately 9.53 mm (3/8 in.) long and 12.7 mm (1/2 in.) wide at the base. Feed rates of  $1.06 \times 10^{-3}$  m/s (2.5 in/min),  $2.54 \times 10^{-3}$  m/s (6.0 in/min) and  $4.23 \times 10^{-3}$  m/s (10.0 in/min) were used. Care was taken to insure that both sides of each slab were sawed at the same feed rate.

2.1.3 Cutting by Milling - These specimens were prepared by first sawing off 14.3 mm (9/16-in.) thick slabs from a 1-gallon block of propellant using the technique and equipment described in Paragraph 2.1.2. The two sides of each slab were then milled, one side at a time, to the desired thickness of 12.7 mm (1/2 in.). An Index Model 645 vertical milling machine specially equipped with an AFRL designed vacuum table vice and a suction vented enclosure (Figure 5) was used. The milling head was shaped like an upside down T rotating about its vertical axis at a speed of 1,000 rpm. The horizontal member of the T was 254 mm (10 in.) long and had a 25.4 mm (1 in.) diameter carbide cutting disk firmly attached to, and near the end of each leg. The slab to be milled was placed on the movable vacuum table vice and firmly held in a fixed position by generating a vacuum at the bottom face of the slab. The vacuum table vice was moved toward the milling head at feed rates of  $0.741 \times 10^{-3}$  m/s (1 3/4 in/min),  $2.01 \times 10^{-3}$  m/s (4 3/4 in/min) and  $3.07 \times 10^{-3}$  m/s (7 1/4 in/min) to obtain a slab at each feed rate. Care was taken to insure that both sides of each slab were milled at the same feed rate.

2.1.4 Cutting by Die Cutter - Three Class C uniaxial tensile test specimens were stamped out from each of the slabs using a Dake manual press with a JANNAF test specimen die cutter attached (Figure 6). Test specimens were clearly marked to identify the slab and position in the slab where each was obtained. They were wrapped in aluminum foil as soon as they were cut and then transported to the test area for testing.

## 2.2 Uniaxial Tensile Test

All uniaxial tensile tests were conducted in accordance with the general guideline provided in Reference 5. Tests were performed using an Instron Model 1123-TS Universal Tester, fitted with a Bemco Model FTU 3.2M Universal Test Machine Temperature Chamber enclosing the test section. Test specimens were cooled by mechanical refrigeration and heating by forced convection of radiant heat from built-in sheath type heaters. The test specimen grips used were of the slip-on type for easy specimen mounting and removal.

Pretest preparation of test specimens usually started with measuring the length and width of the cross-sectional area at the gage section with a dial gage micrometer. The average of three measurements along the gage section at midwidth was used to calculate the cross-sectional area. Test specimens were then placed in predetermined testing order on flat-bottom, custom made aluminum trays. These trays were, in turn, placed inside the temperature conditioning chamber at the desired test temperature for a minimum of 1 hour prior to testing. Test temperature was monitored in the immediate vicinity of the test specimen grips with a platinum/rhodium probe. This probe was used in conjunction with a digital readout unit having 0.1°F resolution. A load cell in axial alignment with the test specimen grips was used to sense the applied tensile force to the test specimen. The load cell and recorders were calibrated with dead weights at each test temperature within each test day.

Each of the properly temperature-conditioned test specimens was tested by slipping it onto the test specimen grips, applying a small preload

(usually less than 1 percent of the expected maximum load), and then pulling it at a preselected constant rate until it was broken. Load cell output was recorded as a function of time on a digital magnetic disk recorder. The same test data was also recorded on a strip chart recorder which provided quick-look and back-up data.

### 2.3 Electron Microscope Surface Examination

Preparation of surface samples to be examined as described in Section 1.2.3 began by cutting 3 mm x 5 mm samples from the islands of propellant slabs (the remaining pieces of a slab from which uniaxial tensile test specimens had been cut out and removed) using a razor blade. Care was taken to correctly identify the surface to be examined, and to record of which cutting method was used for each slab. The samples were then affixed to SEM stubs using Coates and Welter conductive specimen cement. Finally, they were given a light gold coating using a mini-coater manufactured by Film-Vac, Inc.

The face of each properly prepared sample was examined and photographed at magnifications of 30X, 150X and 300X, and an edge (profile) view was photographed at 150X using a Coates and Welter model HPS-70B scanning electron microscope. The HPS-70B has low charging characteristics, real time scanning capabilities, and a capability to map individual elements. The latter capability was used at 150X magnification to facilitate identification of aluminum and ammonium perchlorate particles visible at the surface of the samples. Photographs were taken with a built-in camera and Polaroid 101.6 mm x 127 mm (4 in x 5 in) film, numbers 52, 55 and 57. Both positives and negatives were taken.

## 3. DATA REDUCTION AND ANALYSIS PROCEDURE

### 3.1 Reduction of Uniaxial Tensile Test Data

Recorded force versus time data was partially reduced using a

specialized computer program described in Reference 4. Basically, the points of maximum force, maximum loading rate and rupture were determined directly from the force versus time data as illustrated in Figure 7. The various forces (i.e.  $F_m$ ,  $F_r$  and  $F_e$ ) and their corresponding occurrence times (i.e.  $t_{F_m}$ ,  $t_{F_r}$ , and  $t_{F_e}$ ) were obtained and used to calculate the initial modulus ( $E_0$ ), the stress and strain at maximum force ( $\sigma_m$  and  $\epsilon_m$ ), the stress and strain at rupture ( $\sigma_r$  and  $\epsilon_r$ ) and the area corrected stresses ( $\sigma_{mt}$  and  $\sigma_{rt}$ ).

The remaining part of the data reduction was performed to account for the effects of decreasing test specimen cross-sectional area due to increasing axial strain. The force versus time data were converted to stress ( $\sigma$ ) versus strain ( $\epsilon$ ) using the following relationships:

$$\epsilon_i = \frac{\Delta L_i}{L_g} \quad (1)$$

$$\sigma_i = \frac{F_i}{A_0} (1 + \epsilon_i) \quad (2)$$

where

$\epsilon_i$  is the specimen strain at a particular instant;

$\Delta L_i$  is the change in specimen length at the same instant;

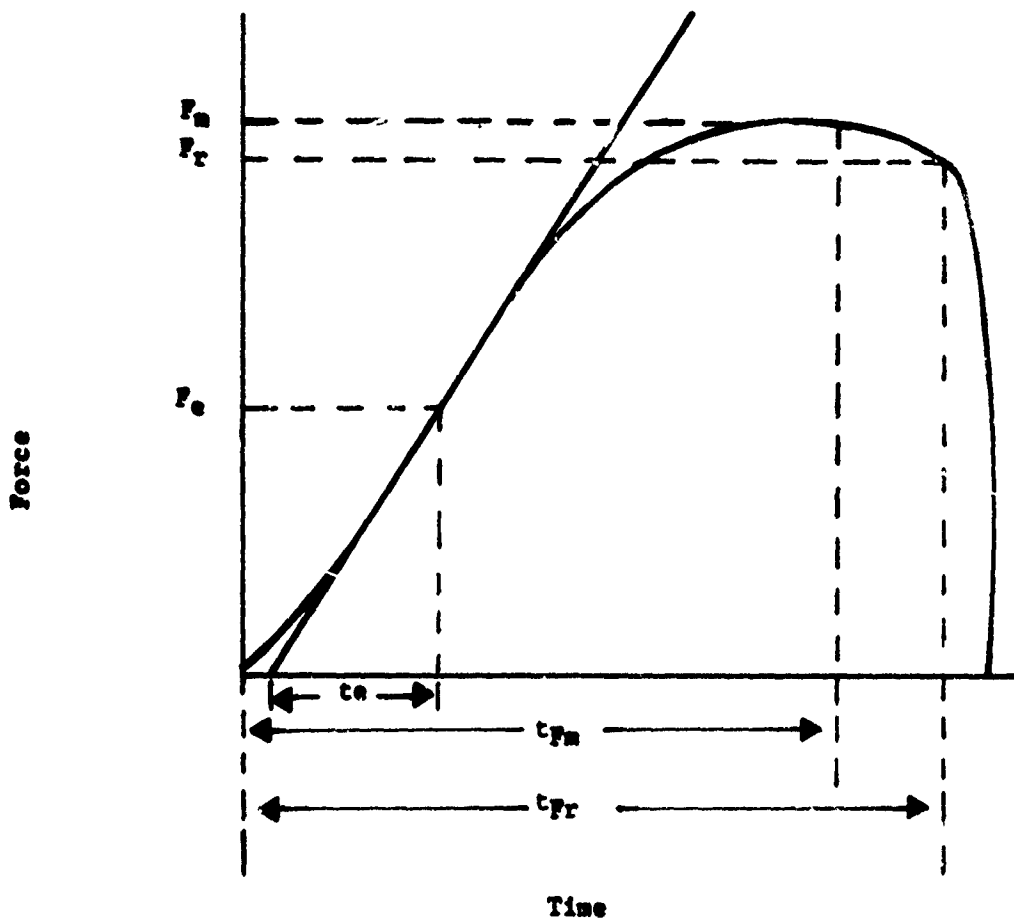
$\sigma_i$  is the specimen stress at the same instant;

$F_i$  is the tensile force on the specimen at the same instant;

$L_g$  is the effective gage length of the test specimen;

$A_0$  is initial cross-sectional area of test specimen.

The converted data may be represented by the graph shown in Figure 8. From this graph, the maximum stress ( $\sigma_{MC}$ ), maximum strain ( $\epsilon_{MC}$ ), rupture



$P_m$  = maximum force.

$P_r$  = rupture force.

$t_{Pm}$  = time from start of the test to the time when the maximum force occurred.

$t_{Pr}$  = time from start of the test to the time when the specimen ruptured.

$P_e$  and  $t_e$  = the force and its corresponding time values selected from the highest tangent for  $E_0$  calculation.

Figure 7. Typical Load-Displacement Curve with Data Reduction Illustration.

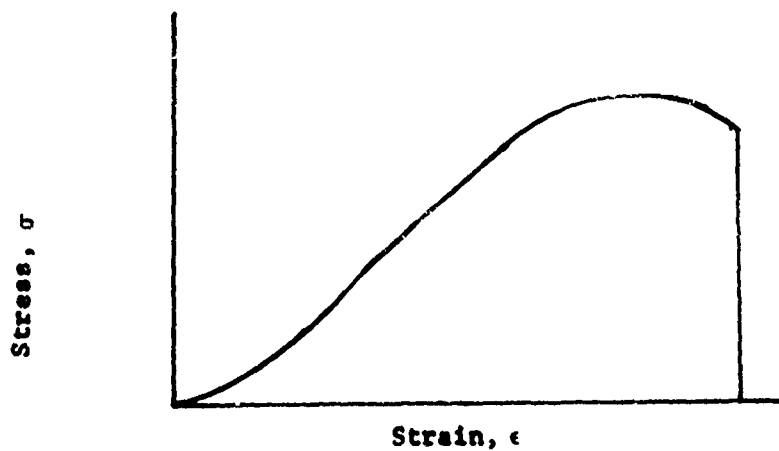


Figure 8. Typical Stress vs. Strain Representation of Test Data

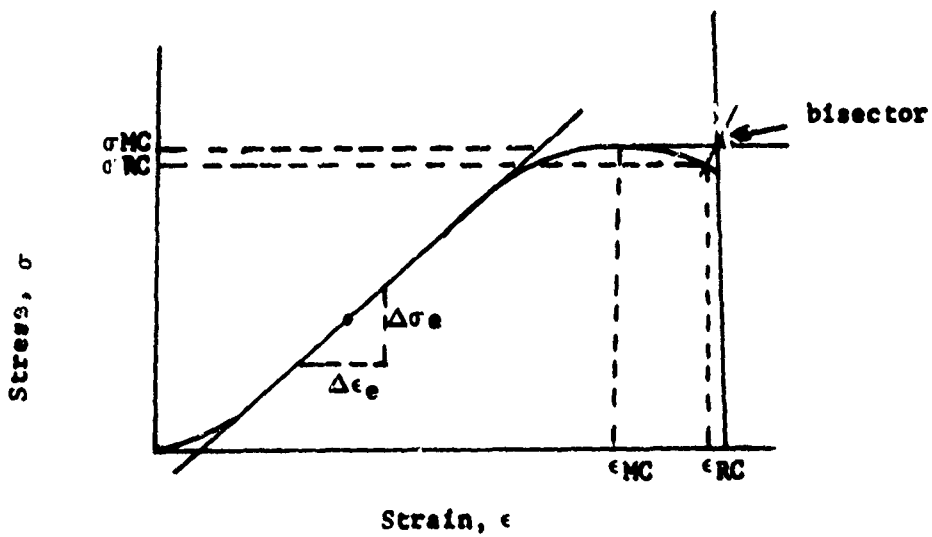


Figure 9. Typical Stress vs. Strain Curve with Data Reduction Illustration

stress ( $\sigma_{RC}$ ) and rupture strain ( $\epsilon_{RC}$ ) were determined as shown in Figure 9. The initial modulus ( $E_{OC}$ ) was obtained by picking out the maximum positive slope from the data curve as shown in Figure 9, and using the equation:

$$E_{OC} = \frac{\Delta\sigma_e}{\Delta\epsilon_e} \quad (3)$$

where  $\Delta\sigma_e$  and  $\Delta\epsilon_e$  define the slope of the tangent to the point of interest.

The effective gage length ( $L_g$ ) used in strain calculations was assigned the value of 68.6 mm (2.7 in.). In reality, the value of  $L_g$  is dependent on the mechanical properties, temperature and strain rate of the propellant. Whenever high accuracy is required, the value of  $L_g$  should be determined experimentally, or wooden tabs for test specimens should be used. The effective gage length may be determined by measuring both the actual strain in the specimen gage section ( $\epsilon_A$ ) and the corresponding crosshead travel ( $D_{xh}$ ), and plugging their values into the following equation:

$$L_g = \frac{D_{xh}}{\epsilon_A} \quad (4)$$

### 3.2 Analysis of Uniaxial Tensile Test Data

Reduced uniaxial tensile test data were analysed for both the influence of cutting speed used in each cutting method and the effect of cutting method on test specimen stress and strain capabilities.

To evaluate influence of cutting speed, the average mechanical properties (stresses, strains and modulus) from the three cutting speeds were calculated first. Then the maximum difference ( $\Delta_{max}$ ) in mechanical

properties between the cutting speeds, were calculated. For each property, this  $\Delta_{max}$  was expressed as a percentage of the average by dividing it by the first calculated quantity. The reduced mechanical properties data were plotted against cutting speed for visual comparison.

To evaluate the effect of cutting method, the reduced data were first corrected for block-to-block variation in mechanical properties. This was necessary because a different block of propellant was used for each cutting method. Using block 1 as the base, the correction factor for each property (i.e., stress, strain, etc) was determined from the control test series described in Section 1.2.4 using the following equation:

$$F_{Px} = \left( \frac{P_1}{P_x} \right) \quad (5)$$

where

$F_{Px}$  is the correction factor for property  $P$  of block  $X$ ;

$P_1$  is property  $P$  of block 1

$P_x$  is property  $P$  of block  $X$ .

Using the corrected data, the following quantities were then calculated:

- (1) Average mechanical properties from the three cutting speeds in each cutting method.
- (2) Average mechanical properties from the three cutting methods.
- (3) Maximum difference ( $\Delta_{max}$ ) in mechanical properties between the cutting methods.
- (4)  $\Delta_{max}$  in mechanical properties between the cutting methods as percent of their average.

The corrected stress and strain data were also plotted against cutting speed for each cutting method.

### 3.3 Analysis of Propellant Surface Photographs

Photographs of cut surfaces were taken with a scanning electron microscope (SEM) at 30, 150 and 300 times magnification. These photographs were visually examined for missing, protruding, dislocated and cracked particles as well as for surface texture and surface profile roughness. The knowledge of the sizes of aluminum and ammonium perchlorate particles, and SEM elemental mapping techniques simplified identification of filler particles visible on cut surfaces. Examination results were tabulated and formatted to compare effects of cutting speeds and cutting methods.

## 4. EXPERIMENTAL RESULTS AND DISCUSSION

### 4.1 Uniaxial Tensile Tests

Uniaxial Tensile test data are summarized in Tables 2 and 3. Table 2 contains original (uncorrected) data and calculated averages of and maximum differences between three cutting speeds within each of the three cutting methods. Table 3 contains the same test data corrected for block-to-block variations in mechanical properties.

In the discussion that follows, emphasis was placed on stress and strain capabilities, especially stress and strain at the maximum load point (i.e.  $\sigma_m$  and  $\epsilon_m$ ). Initial modulus ( $E_0$  and  $E_{OC}$ ) data were not used because the data reduction computer program could not provide an accuracy for this quantity better than  $\pm 10$  percent. Uniaxial tensile properties of solid propellant usually vary from one block of propellant to another and, for a given block of propellant, they vary from slab to slab. The presumably

TABLE 2. UNCORRECTED UNIAXIAL TENSILE TEST RESULTS

SPECIMEN PREPARATION	$E_o$ (MPa)	$\sigma_m$ (MPa)	$\epsilon_m$ (m/m)	$\sigma_r$ (MPa)	$\epsilon_r$ (m/m)	$E_{oc}$ (MPa)	$\sigma_{MC}$ (MPa)	$\epsilon_{MC}$ (m/m)	$\sigma_{RC}$ (MPa)	$\epsilon_{RC}$ (m/m)
<u>MILLING at 1,000 rpm</u>										
0.741 $\times 10^{-3}$ m/s Feed Rate	6.05	.912	.325	.867	.356	7.10	1.21	.344	1.17	.357
2.01 $\times 10^{-3}$ m/s Feed Rate	5.83	.914	.333	.857	.377	7.01	1.22	.353	1.18	.378
3.07 $\times 10^{-3}$ m/s Feed Rate	5.59	.927	.337	.867	.377	6.89	1.24	.355	1.19	.378
Average of 3 Feed Rates	5.82	.918	.332	.864	.370	7.00	1.22	.351	1.18	.371
$\Delta_{max}$ between Feed Rates	0.46	0.15	0.12	.010	0.21	0.21	0.03	.011	0.02	0.21
$\Delta_{max}$ as % of Average	7.9	1.63	3.61	1.16	5.68	3.0	2.46	3.13	1.69	5.66
<u>GUILLOTINE-CUT</u>										
0.414 MPa Pressure	5.05	.888	.337	.839	.375	6.21	1.19	.357	1.15	.375
0.621 MPa Pressure	5.19	.877	.333	.830	.373	6.31	1.17	.353	1.14	.373
0.827 MPa Pressure	5.13	.877	.331	.828	.369	6.34	1.17	.348	1.13	.369
Average of 3 Cut Rates	5.12	.881	.334	.832	.372	6.29	1.18	.353	1.14	.372
$\Delta_{max}$ between Pressures	0.14	.011	.006	.011	.006	0.13	0.02	.009	0.02	.006
$\Delta_{max}$ as % of Average	2.73	1.25	1.80	1.32	1.61	2.07	1.69	2.55	1.75	1.61

TABLE 2. UNCORRECTED UNIAXIAL TENSILE TEST RESULTS (CONT)

<u>SPECIMEN PREPARATION</u>	$E_0$ (MPa)	$\sigma_m$ (MPa)	$\epsilon_m$ (m/m)	$\sigma_r$ (MPa)	$\epsilon_r$ (m/m)	$E_{0c}$ (MPa)	$\sigma_{MC}$ (MPa)	$\epsilon_{MC}$ (m/m)	$\sigma_{RC}$ (MPa)	$\epsilon_{RC}$ (m/m)
<u>SAW-CUT at 350 rpm</u>										
1.06 $\times 10^{-3}$ m/s Feed Rate	6.29	.923	.318	.878	.339	7.72	1.21	.325	1.18	.339
2.54 $\times 10^{-3}$ m/s Feed Rate	5.95	.926	.319	.880	.352	7.48	1.22	.338	1.19	.352
4.23 $\times 10^{-3}$ m/s Feed Rate	6.28	.920	.316	.859	.359	7.64	1.21	.337	1.17	.359
Average of 3 Feed Rates	6.17	.923	.314	.872	.350	7.61	1.21	.333	1.18	.350
$\Delta_{max}$ between Feed Rates	0.34	.006	.011	.021	.020	0.24	0.01	.013	0.02	.020
$\Delta_{max}$ as % of Average	5.51	0.65	3.50	2.41	5.71	3.15	0.83	3.90	1.69	5.71

TABLE 3. CORRECTED UNIAXIAL TENSILE TEST RESULTS

SPECIMEN PREPARATION	$E_0$ (MPa)	$\sigma_m$ (MPa)	$\epsilon_m$ (m/m)	$\sigma_r$ (MPa)	$\epsilon_r$ (m/m)	$E_{DC}$ (MPa)	$\sigma_{MC}$ (MPa)	$\epsilon_{MC}$ (m/m)	$\sigma_{RC}$ (MPa)	$\epsilon_{RC}$ (m/m)
<u>MILLING at 1,000 rpm</u>										
0.741 x 10 <sup>-3</sup> m/s Feed Rate	6.05	.912	.325	.867	.356	7.10	1.21	.344	1.17	.357
2.01 x 10 <sup>-3</sup> m/s Feed Rate	5.83	.914	.333	.857	.377	7.01	1.22	.353	1.18	.378
3.07 x 10 <sup>-3</sup> m/s Feed Rate	5.59	.927	.337	.867	.377	6.89	1.24	.355	1.19	.378
Average of 3 Feed Rates	5.82	.918	.332	.864	.370	7.00	1.22	.351	1.18	.371
<u>GUILLOTINE-CUT</u>										
0.414 MPa Pressure	5.58	.931	.348	.890	.386	6.52	1.27	.390	1.24	.406
0.621 MPa Pressure	5.73	.920	.344	.880	.384	6.62	1.25	.386	1.23	.404
0.827 MPa Pressure	5.67	.920	.342	.878	.380	6.65	1.25	.380	1.22	.399
Average of 3 Cut Rates	5.66	.924	.345	.883	.383	6.60	1.26	.385	1.23	.403

TABLE 3. CORRECTED UNIAXIAL TENSILE TEST RESULTS (CONT)

SPECIMEN PREPARATION	$E_0$ (MPa)	$\sigma_m$ (MPa)	$\epsilon_m$ (m/m)	$\sigma_r$ (MPa)	$\epsilon_r$ (m/m)	$E_{OC}$ (MPa)	$\sigma_{MC}$ (MPa)	$\epsilon_{MC}$ (m/m)	$\sigma_{RC}$ (MPa)	$\epsilon_{RC}$ (m/m)
<u>SAW-CUT at 350 rpm</u>										
1.06 $\times 10^{-3}$ m/s	5.40	.927	.343	.878	.377	6.73	1.26	.378	1.23	.396
Feed Rate										
2.54 $\times 10^{-3}$ m/s	5.11 <sup>9</sup>	.930	.356	.880	.391	6.52	1.27	.393	1.24	.411
Feed Rate										
4.23 $\times 10^{-3}$ m/s	5.39	.924	.352	.859	.399	6.66	1.26	.392	1.22	.419
Feed Rate										
Average of 3 Feed Rates	5.30	.927	.350	.872	.389	6.64	1.26	.388	1.23	.409
<u>COMPARISON OF CUTTING METHODS</u>										
Average of 3 Methods	5.59	.923	.342	.873	.381	6.75	1.25	.374	1.21	.394
$\Delta m_{\max}$ between Methods	0.52	.009	.018	.019	.019	0.40	0.04	.037	0.05	.038
$\Delta m_{\max}$ as % of Average	9.30	0.97	5.30	2.20	5.00	5.90	3.20	9.90	4.10	9.60

small slab-to-slab variation is unknown and was neglected in this work.

A different block of TP-H1011 propellant was used for each cutting method. Similarly, a different slab of propellant from a selected block was used for each cutting speed.

Figures 10 and 11 indicate that the best of the three feed rates for milling, which resulted in highest stress and strain capabilities, appeared to be the highest rate ( $3.07 \times 10^{-3}$  m/s) used. However, the differences in test results between the three rates were very small. For example, the maximum differences in  $\sigma_m$  and  $\epsilon_m$  were only 1.6 and 3.6 percent of their respective average values. Shown in the same figures, the best of the three guillotine operating pressures was the lowest (0.414 MPa) used. However, the maximum differences in  $\sigma_m$  and  $\epsilon_m$  between the three operating pressures used were merely 1.25 and 1.80 percent of their respective average values. Also shown in Figures 10 and 11, the middle feed rate (2.54 MPa) used in the saw-cut method resulted in highest test specimen stress and strain values. Again, the maximum differences in results between the three feed rates were very small (0.65 percent in  $\sigma_m$  and 3.5 percent in  $\epsilon_m$ ).

To compare propellant cutting methods, the block-to-block variation in mechanical properties was evaluated. The results are summarized in Table 4 and plotted in Figures 12 and 13. It is apparent from this data that the variation can be significant. Correction factors ranging from zero to greater than 14 percent were calculated. The corrected data were compared in Figures 10 and 11 and in Table 3. The saw-cut and the guillotine cut test specimens demonstrated slightly higher stress and strain capabilities than did their mill-cut counterparts. The maximum difference between these cutting methods as percent of their average for  $\sigma_m$  and  $\epsilon_m$  were only 0.97 and 5.3 percent, respectively.

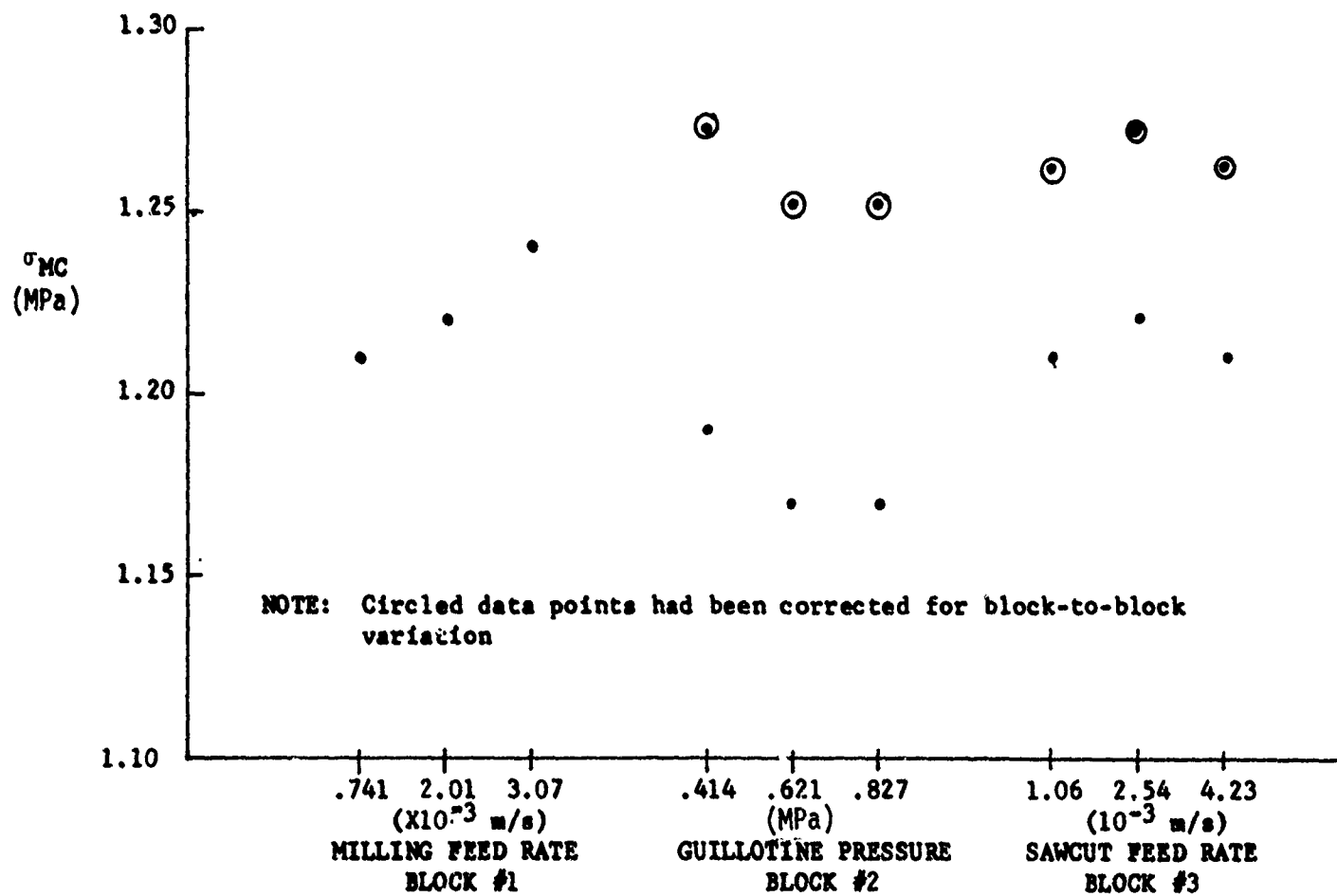
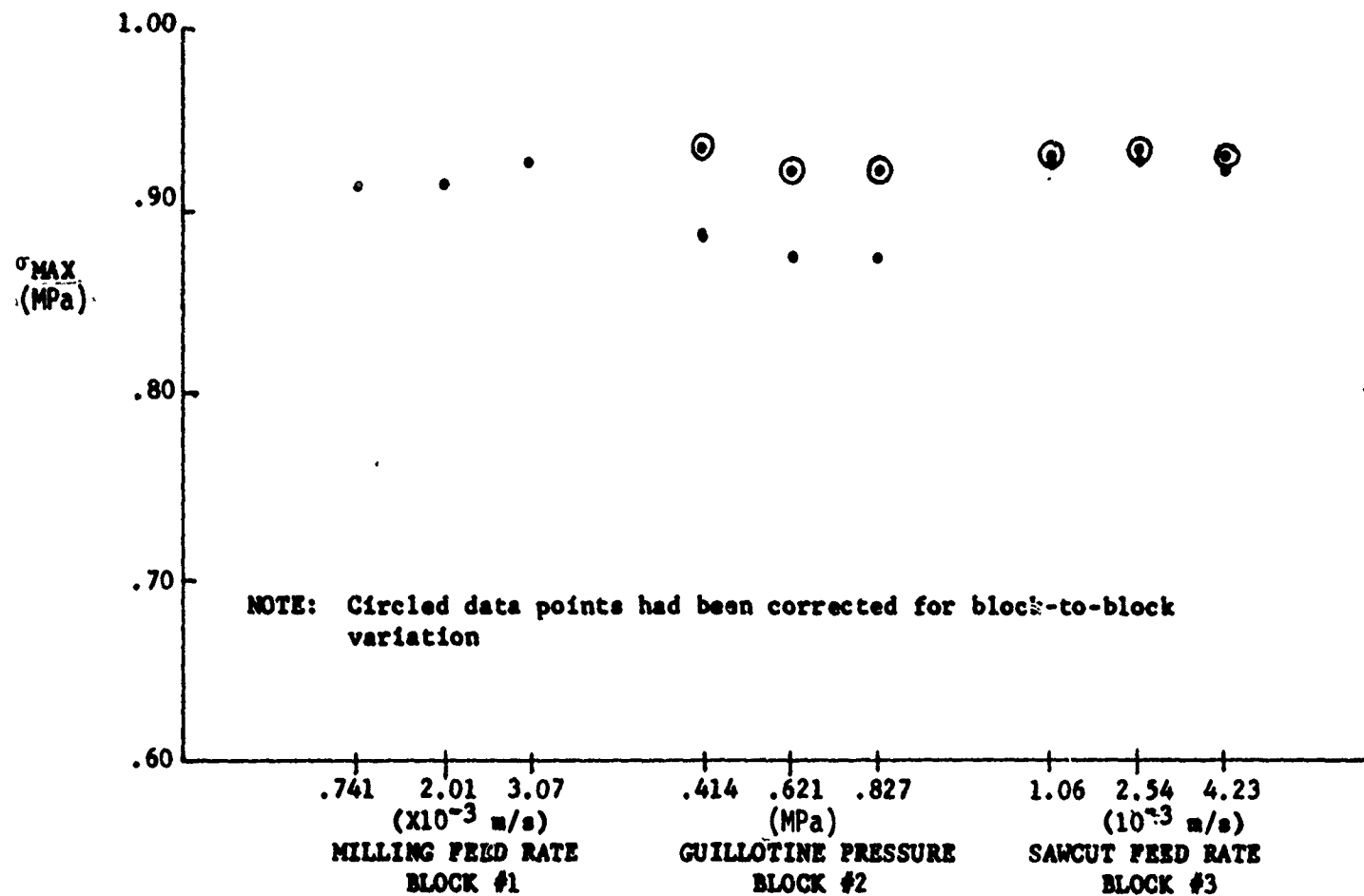


Figure 10. Comparison of Stress Capability Between Cutting Methods and Between Cutting Speeds

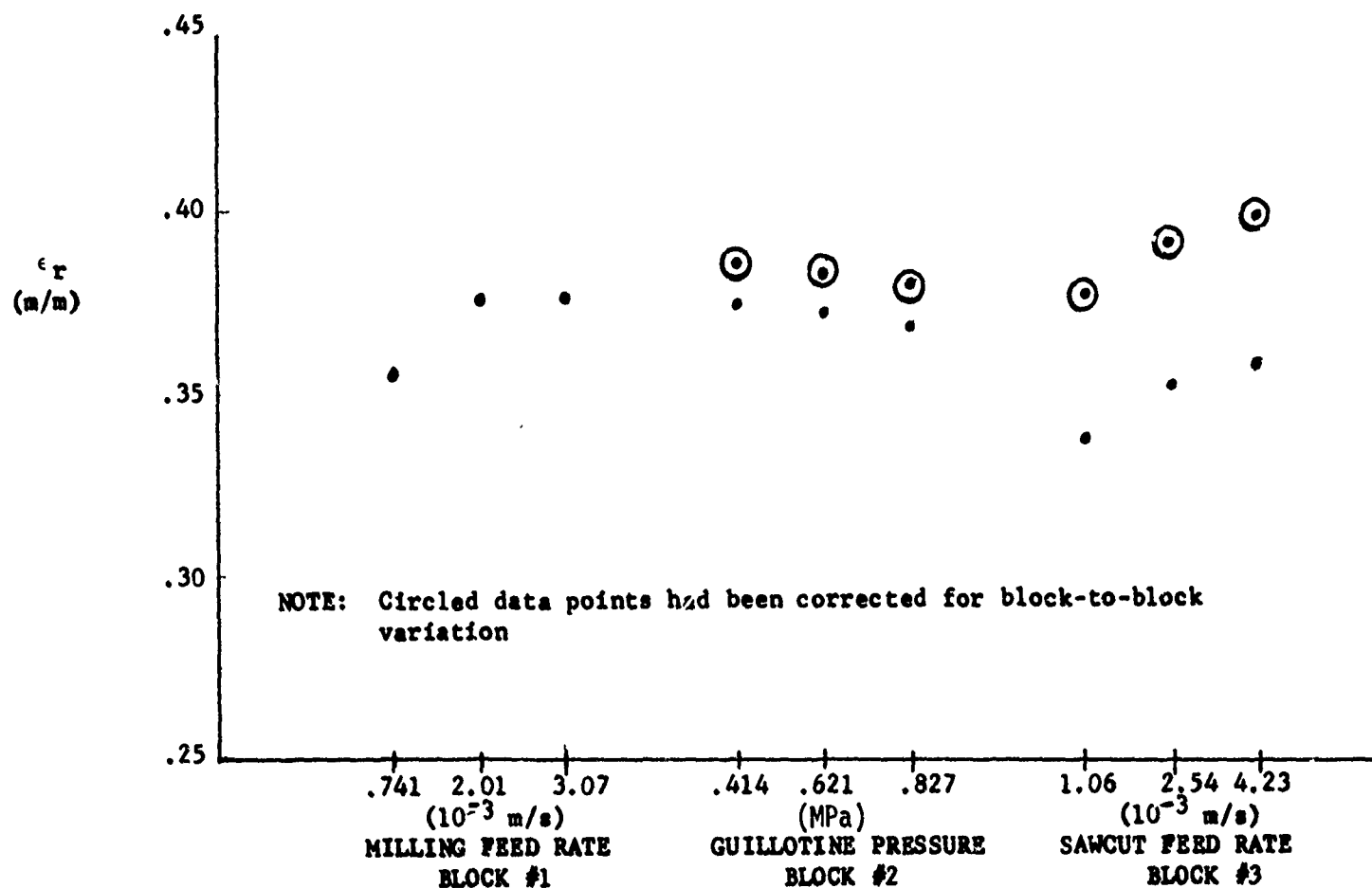
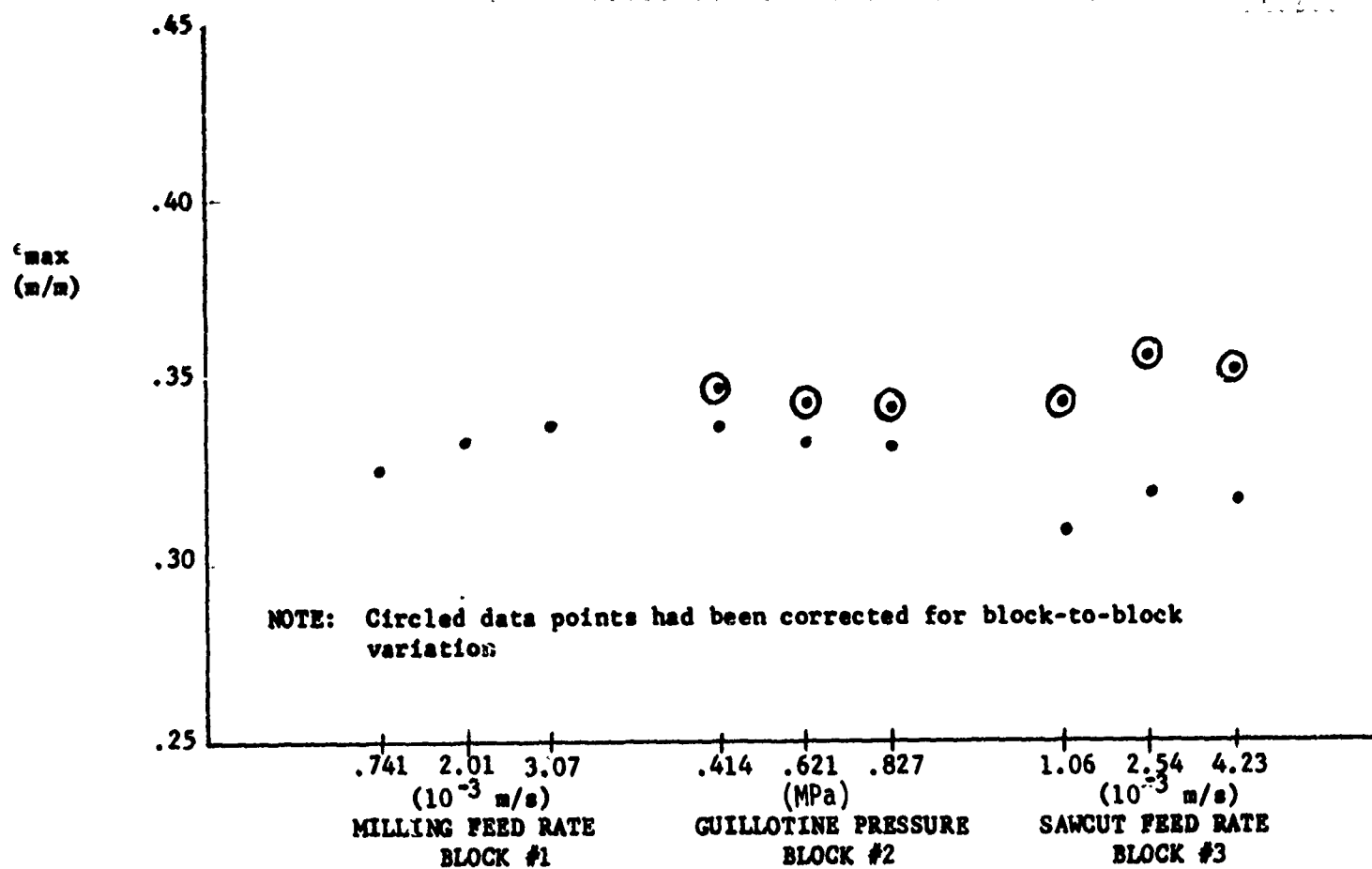


Figure 11. Comparison of Strain Capability Between Cutting Methods and Between Cutting Speeds

TABLE 4. BLOCK-TO-BLOCK VARIATION OF UNIAXIAL  
TENSILE PROPERTIES (MILLING at 1,000 rpm)

PROPELLANT BLOCK NO.	$E_0$ (MPa)	$\sigma_m$ (MPa)	$\epsilon_m$ (m/m)	$\sigma_r$ (MPa)	$\epsilon_r$ (m/m)	$E_{oc}$ (MPa)	$\sigma_{mc}$ (MPa)	$\epsilon_{mc}$ (m/m)	$\sigma_{rc}$ (MPa)	$\epsilon_{rc}$ (m/m)
(1)	5.27	.904	.339	.859	.377	6.79	1.23	.377	1.20	.396
(2)	4.77	.862	.328	.810	.366	6.47	1.15	.345	1.11	.366
(3)	6.14	.900	.304	.859	.339	7.79	1.18	.324	1.15	.339
% Difference between (2) and (1)	-9.15	-4.7	-3.3	-5.7	-2.9	-4.7	-6.5	-8.5	-7.5	-7.6
% Difference between (3) and (1)	16.5	-.4	-10.3	0	-10.1	14.7	-4.1	-14.1	-4.2	-14.4

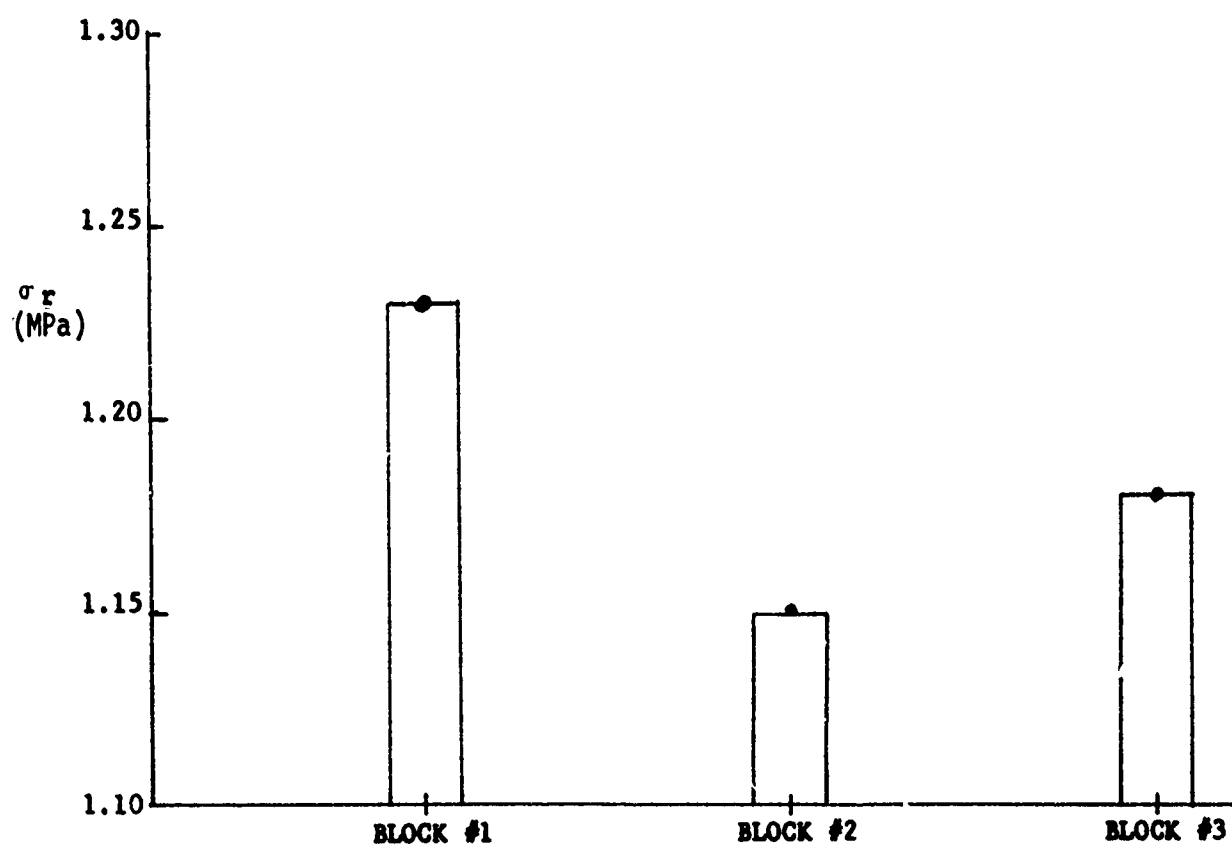
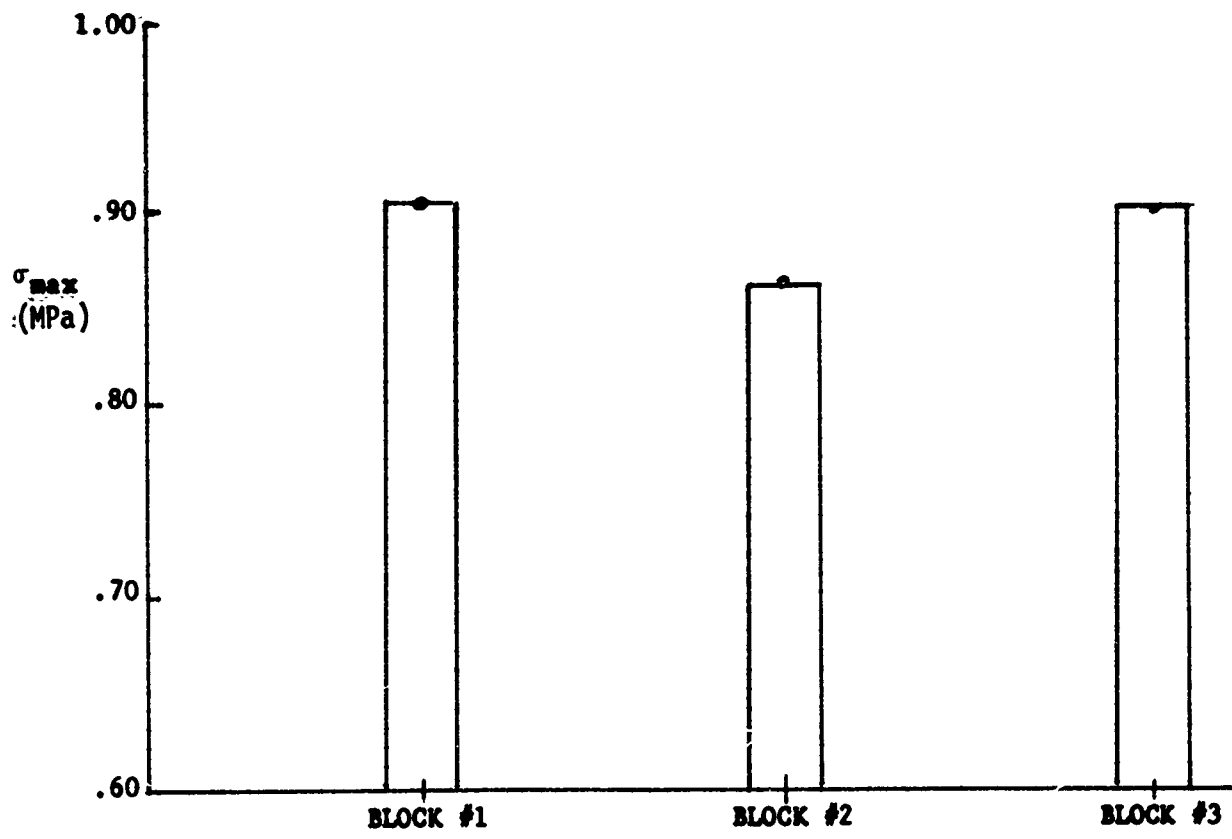


Figure 12. Block-to-Block Variation in Stress Capability

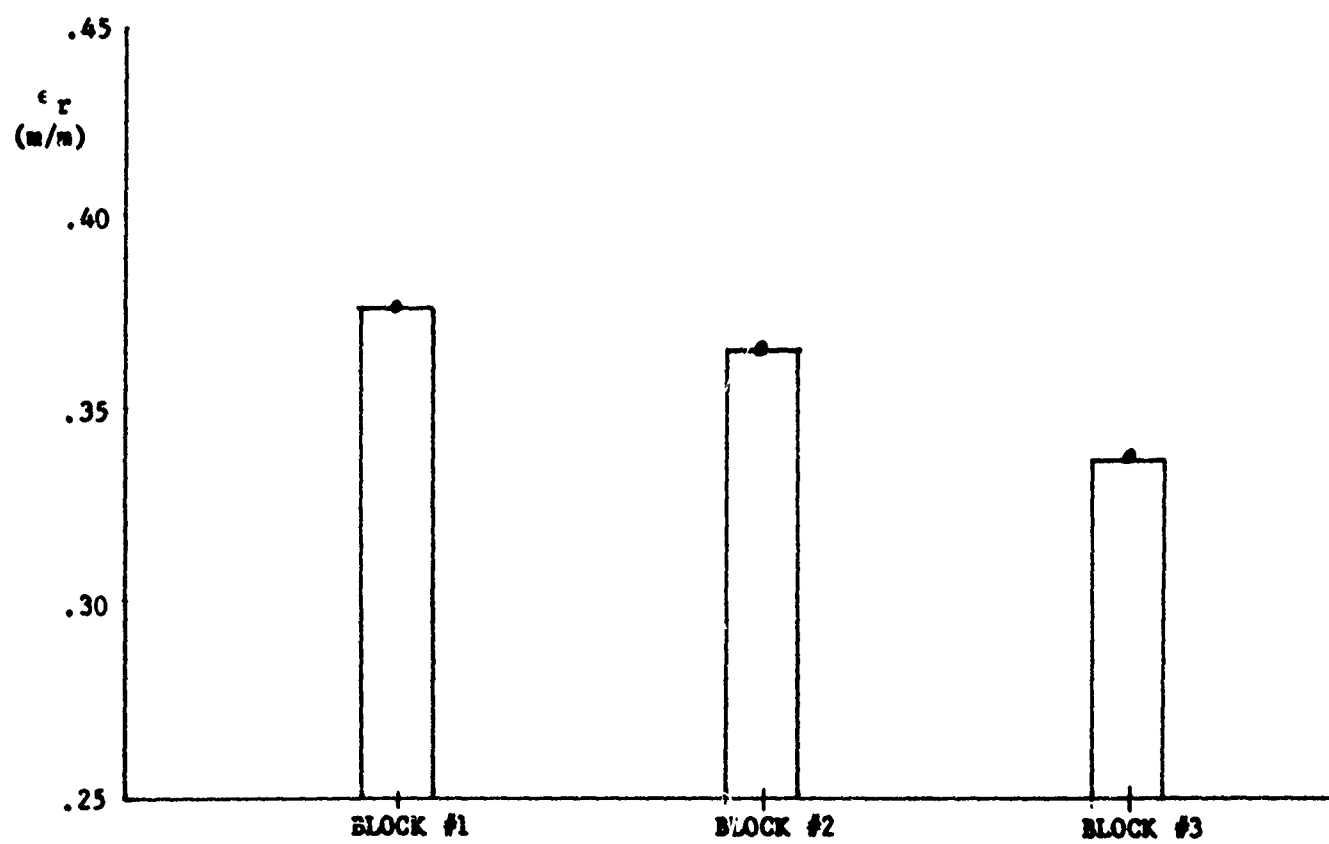
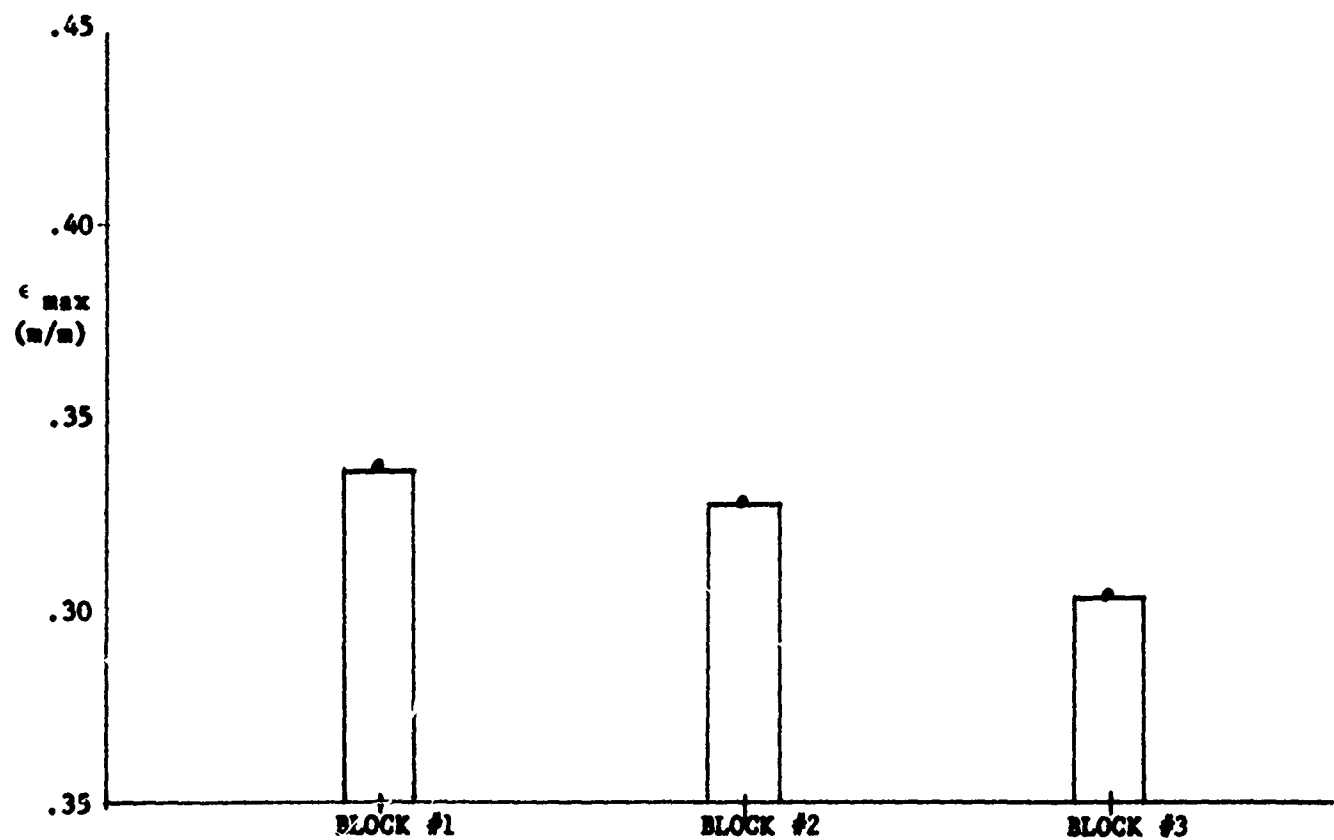


Figure 13. Block-to-Block Variation in Strain Capability

#### 4.2 Electron Microscope Surface Examination

Electron microscope photographs of cut surfaces, which were magnified up to 300 times and included both front and profile (edge) views, are shown in Figures 14 through 22 (rectangles on these photographs identify regions that were further magnified). These photographs were examined for missing, protruding, dislocated and cracked particles as well as for surface texture and surface profile. Results of these examinations are summarized in Tables 5 through 7.

Figures 14 through 16 show that mill-cut surfaces have craters scattered all over and they appear smaller and less distinct at the  $2.01 \times 10^{-3}$  m/s feed rate. This could be the result of either sample-to-sample variation or smearing of binder material over the edges of these craters. Based on particle size, these craters were most likely formed from ammonium perchlorate (AP) particles expelled by the action of the cutter. There was no clear evidence of protruding, dislocated or cracked particles on these surfaces. These surfaces appeared fluffy, which is probably due to smearing of binder material impregnated with very fine particles. As shown in Figures 14d, 15d and 16d, the surface profile at 150X magnification appeared fairly smooth for  $0.74 \times 10^{-3}$  m/s feed rate and became a little rougher at the two higher feed rates.

Magnified photographs of guillotine-cut surfaces are shown in Figures 17 through 19. Three cutting speeds corresponding to operating pressures of 0.414 MPa (60 psi), 0.621 MPa (90 psi) and 0.827 MPa (120 psi) were investigated. Craters were apparent on all cut surfaces, but they appeared fewer in number at the highest cutting speed. Protruding particles were found on all cut surfaces, with higher concentration at the lowest cutting speed. Some evidence of relocated particles and fractured particles

TABLE 5. SEM RESULTS--MILL-CUT SURFACES

Feed Speed	$0.74 \times 10^{-3}$ m/s (1.75 in/min)	$2.01 \times 10^{-3}$ m/s (4.75 in/min)	$3.07 \times 10^{-3}$ m/s (7.25 in/min)
Craters	Many	Many but seem smaller and less distinct	Many
Protruding Particles	No evidence	No evidence	No evidence
Dislocated Particles	No clear evidence	No clear evidence	No clear evidence
Cracked AP	No clear evidence	No clear evidence	No clear evidence
Surface Texture	Fluffy	Fluffy	Fluffy
Surface Profile at 150X	Fairly Smooth	A little rougher	A littler rougher

TABLE 6. SEM RESULTS--GUILLOTINE-CUT SURFACES

Guillotine Operating Pressure	0.414 MPa (60 psi)	0.621 MPa (90 psi)	0.827 MPa (120 psi)
Craters	Many	Many	Few
Protruding Particles	Quite a few	Few	Few
Dislocated Particles	Some evidence; Not conclusive	Some evidence; Not conclusive	Yes
Cracked AP	Some evidence, especially at bottom of craters	Some evidence; especially at bottom of craters	Some evidence; especially at bottom of craters
Surface Texture	Rough	Rough	Rough
Surface Profile at 150 $\lambda$	Rugged	Very rugged	Very rugged

TABLE 7. SEM RESULTS--SAW-CUT SURFACES

	Feed Speed $1.06 \times 10^{-3}$ m/s (2.5 in/min)	2.54 $\times 10^{-3}$ m/s (6 in/min)	$4.23 \times 10^{-3}$ m/s (10 in/min)
Craters	Many	Many	Many
Protruding Particles	Few	No evidence	No evidence
Dislocated Particles	No conclusive evidence	No conclusive evidence	No conclusive evidence
Cracked AP	Not discernible; may be due to photo quality	Not discernible; may be due to photo quality	Not discernable; may be due to photo quality
Surface Texture	Fluffy	Fluffy	Fluffy
Surface Profile at 150X	Fairly smooth	Fairly smooth	Fairly smooth

were also found. Relocated particles were more apparent at the highest cutting speed while fractured particles were equally apparent at all three cutting speeds and were found mostly at the bottom of the craters. Surface texture was generally rough and rocky in appearance for guillotine cuts. Surface profile at 150X magnification also appeared rough and rugged; roughness appeared to increase with cutting speed.

In many respects, saw-cut surfaces are similar to those cut by milling. Magnified photographs of saw-cut surfaces from the three feed rates ( $1.06 \times 10^{-3}$  m/s,  $2.54 \times 10^{-3}$  m/s and  $4.23 \times 10^{-3}$  m/s) are shown in Figures 20 through 22. Craters were again evident on these surfaces. Protruding particles were found only at the lowest feed rate and they were few and far between. Surface texture was generally fluffy. There was no evidence of either cracked particles or dislocated particles; this may be in part caused by the masking effect of fluffy surface texture. Surface profiles from all three feed rates appeared fairly smooth at 150X magnification.

Results of electron microscope examination of propellant surfaces obtained by the three cutting methods are presented in a comparative format in Table 8. All three cutting methods have caused the appearance of craters on cut surfaces. These craters are believed to be formed as the result of large AP particle being expelled by the action of the cutters. The perimeters of these craters were relatively well defined on guillotine-cut surfaces but were fuzzy on both saw-cut and mill-cut surfaces. Some protruding particles were found on guillotine-cut surfaces but not on surfaces cut by the other two methods. Evidence of dislocated particles and cracked particles were confined to guillotine-cut surfaces only. Guillotine-cut surfaces also appeared rough and rugged whereas saw-cut and mill-cut surfaces appeared fluffy. Surface

TABLE 8. SEM RESULTS--COMPARISON BETWEEN CUTTING METHODS

Cutting Method	Guillotine-cut	Saw-Cut	Mill-Cut
Craters	Many; perimeter well-defined	Many; perimeter not well-defined	Many; perimeter not well-defined
Protruding Particles	Some	No significant evidence	No evidence
Dislocated Particles	Some evidence, especially at the highest cut speed	No clear evidence	No clear evidence
Cracked AP	Some evidence, especially at bottom of craters	No clear evidence; may be due to smearing of binder material	No clear evidence; may be due to smearing of binder material
Surface Texture	Rough with protruding particles	Fluffy	Fluffy
Surface profile at 150X	Very rough	A little rough	Rough

profiles at 150X magnification appeared a little rough for saw-cut, rougher for mill-cut and very rough for guillotine-cut.

#### 4.3 Interpretation of Test Results

Magnified electron microscope pictures showed relatively extensive propellant surface damage from cutting with a guillotine. The damage was manifested in extracted, dislocated and fractured AP particles. Because the test propellant did not contain any bonding agent, solid particles (such as AP) were not firmly bonded to the polymeric binder, and the types of surface damage just mentioned should not be expected to significantly affect the stress and strain capabilities of the test specimen. This reasoning is supported by the uniaxial tensile test results which revealed no significant differences in mechanical properties between test specimens prepared using the three cutting methods. These results also infer that damage to nonbonding-agent-containing propellant test specimens is superficial. Similar experiments with bonding-agent-containing propellants may well produce drastically different results.

### 5. CONCLUSIONS AND RECOMMENDATIONS

5.1 Block-to-block variation in propellant uniaxial tensile properties can be significant.

5.2 The differences in uniaxial tensile properties either between the three cutting methods (guillotine-cut, saw-cut and mill-cut) or between the three cutting speeds used in each cutting method are within expected normal data scatter for the type of data involved. Therefore, the differences are insignificant.

5.3 Saw-cut and mill-cut propellant surfaces are similar in appearance and relatively smooth, whereas guillotine-cut surfaces are more rugged and

sustained more damage as manifested in extracted, dislocated and fractured particles.

5.4 No big differences in surface appearance were found between cutting speeds in any of the three cutting methods.

5.5 The absence of bonding agent in the test propellant (TP-H1011) is most likely to be a significant factor in the insensitivity of test specimens mechanical properties to their surface damage condition.

5.6 Conducting a similar effort with a modern propellant formulation, which contains a bonding agent, is recommended.

## 6. REFERENCES

1. Bills, K.W., and Bischel, K.H., "Time-Temperature Superposition Does Not Hold for Solid Propellant Stress Relaxation," JANNAF Structures and Mechanical Behavior Working Group - 14th Meeting, Volume 1, April 1977.
2. Francis, E.C., Murch, S.A., and Peeters, R.L., "Nonlinear Structural Analysis of a Thermal-Loaded Solid Propellant Grain," JANNAF Structure and Mechanical Behavior Working Group - 14th Meeting, Volume II, April 1977.
3. Anderson, G.P., and Suisse, D.C., "Relaxation Modulus Testing of ANB-3066 Propellant," JANNAF Structure and Mechanical Behavior Subcommittee - 15th Meeting, Volumed I, July 1978.
4. Chew, T.J.C., Stacer, R.G., and Biggers, R.A., "Aging and Storage Methods Evaluation of Reduced Smoke Propellants for the Maverick Motor," Air Force Rocket Propulsion Laboratory, AFRPL-TR-79-56, October 1979.
5. "Solid Propellant Mechanical Behavior Manual". Chemical Propulsion Information Agency Publication No. 21 (U), Section 4.3.2, November 1970.